HHS Public Access

Author manuscript

Shock. Author manuscript; available in PMC 2017 February 01.

Published in final edited form as:

Shock. 2016 February ; 45(2): 148–156. doi:10.1097/SHK.0000000000000507.

System-wide Mapping of Activated Circuitry in Experimental Systemic Inflammatory Response Syndrome

Sina A. Gharib, MD[1,2,3,4], **Daniel Mar**[4], **Karol Bomsztyk, MD**[4], **Oleg Denisenko, PhD**[4], **Shireesha Dhanireddy, MD**[4], **W. Conrad Liles, MD PhD**[2,4], and **William A. Altemeier, MD**[2,3,4]

[1]Computational Medicine Core, University of Washington, Seattle WA

[2]Center for Lung Biology, University of Washington, Seattle WA

[3]Division of Pulmonary and Critical Care Medicine, University of Washington, Seattle WA

[4]Department of Medicine, University of Washington, Seattle WA

Abstract

Sepsis-induced multiple organ dysfunction syndrome (MODS) is a major cause of morbidity and mortality in critically ill patients and remains impervious to most therapeutic interventions. We utilized a clinically relevant murine model of systemic inflammatory response syndrome (SIRS) during early MODS induced by ventilator-associated pneumonia to systematically delineate pathways dysregulated in lung, liver, and kidney. We focused on processes commonly activated across at-risk organs and constructed a SIRS-associated network based on connectivity among the gene members of these functionally coherent pathways. Our analyses led to the identification of several putative drivers of early MODS whose expression was regulated by epidermal growth factor receptor. Our unbiased, integrative method is a promising approach to unravel mechanisms in system-wide disorders afflicting multiple compartments such as sepsis-induced MODS, and identify putative therapeutic targets.

Keywords

sepsis; organ dysfunction; gene expression; network; microarray

INTRODUCTION

Sepsis—a systemic inflammatory response syndrome (SIRS) caused by an infection—is categorized as severe when complicated by the presence of multi-organ dysfunction (1). Severe sepsis represents a major health burden worldwide, and in the United States alone, there are an estimated 750,000 cases resulting in 215,000 deaths annually with a cost of approximately $17 billion (2). Significant research has been devoted to understanding the pathobiology of sepsis and multiple organ dysfunction syndrome (MODS). To date, the majority of efforts have focused on the hyper-inflammatory state based on circulating markers seen in sepsis; however, clinical trials targeting this pro-inflammatory state through

Corresponding author: Sina A. Gharib, MD, Box 358052, 850 Republican St., Seattle, WA 98109, sagharib@u.washington.edu, Tel: 206-221-0630, Fax: 206-221-0739.

either non-specific inflammatory suppression with corticosteroids or through targeted disruption of pro-inflammatory signaling pathways have been uniformly unsuccessful (3, 4). Because MODS is also associated with widespread microvascular thrombosis, several clinical trials have evaluated disruption of coagulation pathways; however, none of the tested interventions resulted in a significantly improved outcome (5, 6). Although recent pre-clinical studies have suggested a possible therapeutic benefit with mesenchymal stromal (stem) cell therapy (7, 8), the mechanisms, long-term sequelae, and benefits in human disease have yet to be determined. In summary, sepsis-induced MODS remains a significant clinical problem for which no effective pharmacologic strategies other than antimicrobial therapy have been identified.

To better understand the pathogenic mechanisms of multiple-organ dysfunction in sepsis, we previously developed a murine model of MODS by combining *Staphylococcus aureus* pneumonia with mechanical ventilation (MV+SA) that resulted in extra-pulmonary organ injury, i.e., renal and hepatic dysfunction, in the absence of disseminated *S. aureus* infection (9). Within 6 hours of exposure to MV+SA, mice develop profound SIRS with significant elevation in plasma levels of IL-6, KC and MIP-2. An analogous clinical syndrome, ventilator-associated pneumonia (VAP), is an important cause of MODS in critically ill patients with an incidence of 2-16 episodes per 1000 ventilator-days and an attributable mortality of 3-17% (10). The most commonly identified pathogen in VAP is *S. aureus*, occurring in an estimated 28% of cases (11). Therefore, our murine model of VAP-induced MODS captures many of this complex clinical syndrome's salient features.

The present study was designed to test our hypothesis that MODS is preceded by the early activation of a common core of functionally coherent pathways across injured organs, and that these pathways are regulated by a limited set of genes whose identification may lead to novel therapeutic targets. Experimental SIRS was induced in mice subjected to a combination of *S. aureus* pneumonia and mechanical ventilation, and the transcriptional responses of lung, liver, and kidney were interrogated before the onset of overt organ failure. We have previously shown that a longer duration of this animal model leads to significant dysfunction in these key organs (9). Using pathway enrichment and network analysis, we mapped organ-spanning biologic modules activated in SIRS and identified putative critical control sites in this systemic syndrome.

MATERIALS AND METHODS

Animal experiments

The Office of Animal Welfare at the University of Washington approved all experiments. *S. aureus* (SA) was prepared and mice were inoculated and mechanically ventilated as previously described (9). Briefly, for each experiment, a frozen aliquot of methicillin-sensitive *S. aureus* originally isolated from a bacteremic patient was thawed and cultured on a sheep blood agar plate. The following morning, a single colony was selected and cultured overnight at 37°C in tryptic soy broth. The following morning, the bacteria were washed twice with saline and then resuspended in 2 mL of filtered, distilled water. Serial log dilutions were made and turbidity measured by OD_{540}. Using a standard curve generated

previously with OD_{540} versus bacterial concentration determined by quantitative culture, a working solution of ~2×10^8 ± 10% was prepared with filtered, distilled water.

For each experiment, mice were anesthetized with 5% isoflurane and suspended by the front teeth at a 60° angle. The tongue was extruded with forceps and 50 μL of *S. aureus* (~10^7 cfu) was deposited in the oropharynx. Mice in the non-ventilated, SA only group (n = 5) were returned to their cages, monitored for recovery from anesthesia and then allowed free access to food and water. Mice in the combined mechanical ventilation and *S. aureus* pneumonia (MV+SA, n = 5) group were place on a nose cone with 5% isoflurane and intubated via tracheostomy with a 20 gauge blunt metal catheter. Intubated mice were connected to a MiniVent rodent ventilator (Harvard Biosciences, Hollison, MA) and mechanically ventilated with a tidal volume of 10 mL/kg, a respiratory rate of 150 breaths per minute, FiO_2 of 0.21, and no end-expiratory pressure. Anesthesia was maintained with isoflurane (1-1.5%). Neuromuscular blockade was induced with pancuronium (0.02 mg in 0.2 mL s.q.). A second dose of pancuronium (0.01 mg in 0.1 mL) was given after 2 hours. Control mice (n = 5) were maintained in their cages and given an equivalent volume of PBS subcutaneously at times 0 and 2 hours. After 6 hours, mice were deeply anesthetized with 5% isoflurane and euthanized by cardiac puncture and exsanguination. Lungs, kidneys, and livers were immediately recovered for subsequent RNA isolation and analysis.

RNA isolation

For each organ, total RNA was obtained using RNeasy Mini Kit (Qiagen, Valencia, CA) according to the manufacturer's protocol. For microarray experiments, integrity of purified total RNA samples was assessed qualitatively using an Agilent 2100 Bioanalyzer (Agilent Technologies, Santa Clara, CA).

Microarray experiments

Total RNA from each sample was hybridized to a Mouse Genome 430 2.0 microarray (Affymetrix, Inc., Santa Clara, CA) that measures expression levels of over 34,000 well-characterized mouse genes. Gene expression levels from probe intensities were estimated using the robust multiarray analysis (RMA) method with quantile normalization and background adjustment (12). Three samples (n = 2 control livers, n = 1 control lung) did not meet strict hybridization QC criteria and were not subsequently analyzed. To assess organ- and experimental-specific contributions to variability in global gene expression, multidimensional scaling using correspondence analysis was applied across all lung, liver and kidney samples during MV+SA and control conditions (13). For this analysis, the RMA normalization procedure was applied to all samples. However, we observed that organ-specific gene expression dominated the overall transcriptional profiles. Therefore, we implemented RMA separately for each organ (liver, lung, kidney) for subsequent analyses. Detailed microarray experiment description, meeting Minimum Information About a Microarray Experiment (MIAME) criteria, is available at Gene Expression Omnibus (GSE60088).

Differential gene expression

Organ-specific differential gene expression (MV+*SA vs.* control), was determined using a Bayesian implementation of the parametric *t*-test (14) coupled with false discovery rate (FDR) analysis based on Benjamini-Hochberg (15) adjustment of *P*-values. An adjusted *P*-value < 0.01 was used to identify significant differential gene expression.

Gene set enrichment analysis (GSEA)

For each organ, control and MV+SA global expression profiles were imported into GSEA program and analyzed using gene set permutation analysis of 1320 curated pathways as compiled by domain experts from KEGG (http://www.genome.jp/kegg), BioCarta (http://www.biocarta.com), and Pathway Interaction Database (http://pid.nci.nih.gov) among others (16). We used a false discovery rate threshold < 5% to identify significantly enriched pathways and performed leading edge analysis to identify the pathway-associated genes driving the transcriptional response to MV+SA. We grouped enriched pathways based on their leading gene membership profiles using hierarchical clustering to identify biologic modules defined as larger aggregations of overlapping processes.

Network analysis

Leading edge genes mapping to distinct modules representing select group of functionally coherent pathways that were differentially activated across all three organs were linked together based on published gene product interaction databases (17, 18). To increase confidence in the biological relevance of gene-gene connections, we limited the type of interaction to experimentally verified direct relationships (e.g., physical binding between two gene products).

Quantitative PCR analysis (qPCR)

To validate differential expression of select candidate genes, independent experiments on 12 mice (n = 6 MV+SA, n = 6 Control) were performed and lungs, kidneys, and livers harvested. RNA was extracted from flash frozen tissue fragments using Trizol reagent as per the manufacturer's protocol. RNA quantity and purity was assessed, using a Nanodrop 1000 spectrophotometer (Thermo Scientific, Wilmington, DE). To synthesize cDNA, 400 ng of Trizol-extracted total RNA was reverse transcribed with 200 units MMLV reverse transcriptase (Invitrogen, Carlsbad, CA) and random hexamer primers in 20 μl reactions. All PCR reactions were run in quadruplicates. PCR calibration curves were generated for each primer pair from a dilution series of total mouse genomic DNA. The PCR primer efficiency curve was fit to cycle threshold (C_t) versus Log [genomic DNA concentration] using an R-squared best fit. mRNA level of a given gene in each sample was normalized to β-actin transcript.

Evaluation of exogenous EGF on gene expression during early MODS

Mouse epithelial growth factor (EGF) isolated was obtained as a lyophilized solid from Harlan Laboratories. A stock solution of 1 mg/mL in sterile 0.9% saline was prepared and stored in aliquots at −2°C. For each experiment, one aliquot was thawed and diluted to 0.1 mg/mL with sterile 0.9% saline. Twelve C57BL/6 mice were randomized to receive either

0.1mg/kg of EGF (n = 6) or an equivalent volume (1 mL/kg) of sterile 0.9% saline intraperitoneally (n = 6). Thirty minutes after receiving either EGF or saline control, all mice were subjected to *S. aureus* lung infection and mechanical ventilation as described above. At the conclusion of mechanical ventilation, mice were killed and organs collected for RNA isolation and analysis.

RESULTS

Organ-specific gene expression profiles dominate the transcriptional landscape at baseline and after injury

To compare the effects of exposure and organ type on gene expression variability, we performed multidimensional scaling using correspondence analysis on all available samples (n = 27). For this analysis, gene expression values were normalized across all samples. As shown in Figure 1, the most important determinant of sample segregation was organ type (lung, liver, kidney), followed by exposure (MV+SA vs. control). As expected, biologic replicates clustered closely together. Based on this observation, we opted to study each organ separately by comparing organ-specific responses to MV+SA. This approach avoided the substantial adjustments forced by normalizing gene expression values across heterogeneously responsive organs.

MV+SA induces significant transcriptional perturbations in multiple organs

Six hours of exposure to MV+SA caused profound changes in gene expression across all three organs: 4618 unique genes in lung, 1139 unique genes in kidney, and 524 unique genes in liver were differentially expressed during the development of SIRS (adjusted *P*-value < 0.01) (Supplementary Figure S1). Whereas the robust transcriptional changes observed in the lung was anticipated, we found that combining mechanical ventilation with *S. aureus* pneumonia caused a synergistic increase in the number of differentially expressed genes in extra-pulmonary organs (Supplementary Figure S2).

SIRS is characterized by the enrichment of common and divergent pathways across organs

To identify pathways affected by our experimental model of SIRS, we applied GSEA to transcriptional profiles of lung, liver and kidney. We limited the selection of pathways to those derived from expertly-curated domains (n = 1320) and imposed a strict FDR < 5% to denote significant enrichment. Furthermore, we focused our attention on genes whose expression differences drove the enrichment score of a given gene set, an approach known as leading edge analysis (16). As summarized in Figure 2, our results revealed several distinct enrichment patterns across organs in response to MV+SA. Most gene sets were comprised of up-regulated genes during SIRS (red boxes, Figure 2), with lung having the largest number of enriched gene sets (n = 223). Many pathways were enriched selectively in each organ, highlighting the diverse, organ-specific molecular responses induced by systemic inflammation (complete list is available in Supplementary Table S1). Importantly however, we also identified a number of shared pathways in all three organs. This finding implies that SIRS activates a common core of processes across organs and provided an

opportunity to discover putative effectors of the system-wide response to multi-organ dysfunction.

Integration of GSEA and network analysis identifies co-regulated pathways and candidate targets in SIRS

The SIRS-induced gene sets common to lung, liver and kidney included approximately 450 leading edge genes (Figure 3). We clustered these pathways based on their gene membership profile to identify larger, functionally related biologic "modules". We found that the pathways segregated into several distinct modules. The largest grouping included the "signaling in immune system" gene set and a number of associated pathways including innate immunity, Toll receptor cascade, TNF signaling, MAP kinase pathway, and NF-κB/Rela signaling (SIRS-associated Module 1, Figure 3). We confirmed differential up-regulation of several key members of these pathways (*Tlr2*, *Tlr4*, *Tnfa*) across organs during MV+SA using qPCR in an independent set of animal experiments (Figure 4). Given the size and functional profile of Module 1's gene sets, it is likely a dominant player in multi-organ response during SIRS.

However, since the role of many processes in this immuno-inflammatory module has been extensively studied in sepsis, we focused our attention on another distinct module, as highlighted in Figure 3 (SIRS-associated Module 2), that was comprised of interleukins, epidermal growth factor (EGF), platelet-derived growth factor, thrombopoietin, and Jak-STAT signaling pathways. To elucidate the relationship among members of Module 2, we exploited experimentally verified gene product interaction databases (17, 18) and constructed a relational network populated by leading edge genes (Figure 3, Supplementary Table S2). This network was built from 113 nodes (genes) and 713 edges (direct interactions) and was characterized by several densely connected hubs, including epidermal growth factor receptor (EGFR), signal transducer and activator of transcription 3 (STAT3), jun proto-oncogene (JUNB), and interleukin-6 (IL6). We noted that IL6 and JUNB were members of both Module 1 and Module 2 suggesting some intermodular overlap between nodes. Differential upregulation of these four representative genes in lung, liver and kidney during SIRS was confirmed with qPCR in an independent set of animal experiments (Figure 4).

In our computationally derived SIRS-associated Module 2, the most highly connected node was EGFR, suggesting that the EGF pathway may represent a key regulator of pan-organ transcriptional responses in early MODS (Figure 3). If the EGF-EFGR axis is a key regulator of the initial system-wide response to organ dysfunction, we postulated that its influence should span across other activated modules, in particular, Module 1.

Exogenous murine EGF suppresses key immuno-inflammatory genes in SIRS

We investigated the organ-specific transcriptional effects of targeting the EGF-EGFR axis by treating mice during MV+SA with murine EGF (mEGF) and assessing the expression of several key up-regulated members of the immuno-inflammatory MODS-associated Module 1. We found that mEGF significantly down-regulated the expression of *Tlr2*, *Tlr4* and *Tnfa* in lung and kidney during MV+SA (Figure 5). To comprehensively map the relationship

between the EFG-EFGR axis and Module 1, we applied network analysis between EGFR (the Module 2 hub) and the 337 nodes of Module 1. EGFR directly interacted with many members of this module including *Tlr2*, *Tlr4*, and *Tnfa* (Figure 6). This finding implies that the EGF-EGFR pathway modulates a large repertoire of SIRS-associated genes and pathways across at-risk organs.

DISCUSSION

SIRS is the key initial host response preceding multiple organ dysfunction—a syndrome that is a leading cause of death among critically ill patients and without effective pharmacologic therapy. We postulated that since MODS afflicts multiple sites, shared molecular mechanisms across injured organs during SIRS are likely to be critical drivers of this system-wide syndrome and represent logical targets for therapy. Using a clinically relevant animal model of early MODS, we mapped activated pathways within and across lung, liver and kidney, and identified functionally cohesive biological modules and networks common to these at-risk compartments.

The utility of murine models for mimicking human systemic inflammatory disorders such as sepsis has recently been questioned in a widely referenced publication (19). However, that study was based on weak correlations observed between gene expression profiles of circulating leukocytes in acute inflammatory human diseases versus their corresponding mouse models, and did not compare organ-specific responses. Furthermore, some of the statistical approaches used in that paper have been recently criticized (20). The failure of pharmacologic therapies in severe sepsis may reflect the fact that most target candidates have been selected from circulating markers instead of at-risk compartments. Our study demonstrates that SIRS elicits distinct end organ transcriptional signatures (Figures 1 and 2), implying that site-specific targeting may be crucial for improving outcomes in systemic inflammatory states. For example, the single most effective intervention to reduce mortality in critically ill patients with acute respiratory distress syndrome is lung protective ventilation (21). However, tailored therapy for multiple compartments in systemic disorders such as MODS is challenging and impractical—a limitation that motivated us to search for common pathways activated across at-risk organs. Early targeting of key control sites within these shared pathways may lead to beneficial systemic effects by simultaneously reducing injury in multiple organs.

Exploiting an unbiased bioinformatics approach, we identified several SIRS-associated biologic modules. The largest module was comprised of many well-recognized pathways involved in the immune response to sepsis such as Toll-like receptors, TNF pathway, and NF-κB signaling cascade. We chose to also investigate another module that included the EGF signaling axis because the role of this pathway in MODS is less understood. We found that the topology of its corresponding network was centered on EGFR, a densely connected hub that in turn interacted with several other nodes including JUNB, STAT3, and IL6 (Figure 3). There is increasing evidence that the functional integrity of biologic networks is critically dependent on such richly interacting nodes (22-24). Intriguingly, targeting Module 2's EGF-EGFR using exogenous murine EGF lead to the down-regulation of several key genes in pathways mapping to the larger Module 1 including *Tlr2*, *Tlr4*, and *Tnfa*. This

intermodular relationship was systematically highlighted by network analysis that revealed widespread interaction between EGFR (a Module 2 hub) and many members of multiple SIRS-associated pathways in Module 1 (Figure 6).

Although a growing body of evidence supports an important role for epidermal growth factor receptor signaling in mediating liver (25), kidney (26) and lung-specific (27, 28) injury, there is a paucity of reports on its contribution to the development of MODS in critical illness. Coopersmith *et al* studied the role of systemic administration of EGF in improving gut integrity using murine models of sepsis and demonstrated reduced gut injury and mortality in treated animals (29, 30). The widespread availability and clinical use of EGFR inhibitors as anti-neoplastic therapies provides future opportunities to explore the functional role of this SIRS-associated network hub in severe sepsis through direct pharmacologic targeting. Interestingly, inhibition of the EGF-EGFR axis using anti-EGFR monoclonal antibodies is associated with increased risk of severe infections in cancer patients (31), further implicating this pathway as a key regulator of host response to sepsis. Furthermore, several other network nodes identified from our analysis are druggable sites, further supporting the utility of our approach in systematically identifying new therapeutic targets in MODS (please see Supplementary Table S2).

Our study has a number of limitations. We relied on transcriptional profiling, but differential gene expression does not necessarily correlate with changes in protein abundance. Future studies integrating proteomic and metabolomic measurements with gene expression signatures in at-risk organs will provide deeper insights into the complex mechanisms leading to MODS. Our mouse model of early MODS, while clinically relevant, has significant differences with other widely used models such as cecal ligation and puncture (CLP). Importantly, our animal model was based continuous mechanical ventilation, which is common in critically ill patients but precluded long-term exposure. We interrogated global gene expression at a single early time point and therefore did not capture dynamic changes in gene expression (32). A comprehensive investigation across multiple time points and various animal models of SIRS and MODS will allow more generalizable conclusions. However, the focus of this work was elucidation of transcriptional programs preceding the onset of overt organ dysfunction, and our approach using an early 6-hour time point identified many differentially expressed genes and pathways. We depended on curated pathway resources and gene product interaction databases to create MODS-associated networks—but these knowledgebases are incomplete and subject to change. Furthermore, to minimize false positive associations, we limited network relationships to experimentally validated direct gene product interactions and therefore did not capture potentially important indirect influences across genes. Finally, an important limitation of our study is its reliance on a murine model of early MODS. Clearly, future studies are needed to assess whether our findings are biologically relevant in sepsis-induced organ dysfunction in humans.

In summary, we developed a framework to systematically map commonly activated pathways and networks across compartments during SIRS and early onset of experimental MODS. Our results identified *Egfr* as a putative universal integrator of end organ responses in this syndrome, and a promising target for influencing its adverse consequences. Future

studies will be needed to unravel the role of these computationally derived candidates in multiple organ dysfunction of critical illness.

Supplementary Material

Refer to Web version on PubMed Central for supplementary material.

ACKNOWLEDGEMENTS

The authors would like to thank Ms. Dowon An for expert technical assistance.

Funding: This project was supported in part by National Institutes of Health grants HL073996, HL086883, HL122895, DK083310, GM111439, and CA191135.

REFERENCES

1. Levy MM, Fink MP, Marshall JC, Abraham E, Angus D, Cook D, Cohen J, Opal SM, Vincent JL, Ramsay G. 2001 SCCM/ESICM/ACCP/ATS/SIS International Sepsis Definitions Conference. Crit Care Med. 2003; 31(4):1250–6. [PubMed: 12682500]
2. Angus DC, Linde-Zwirble WT, Lidicker J, Clermont G, Carcillo J, Pinsky MR. Epidemiology of severe sepsis in the United States: analysis of incidence, outcome, and associated costs of care. Crit Care Med. 2001; 29(7):1303–10. [PubMed: 11445675]
3. Deans KJ, Haley M, Natanson C, Eichacker PQ, Minneci PC. Novel therapies for sepsis: a review. J Trauma. 2005; 58(4):867–74. [PubMed: 15824673]
4. Tidswell M, Tillis W, Larosa SP, Lynn M, Wittek AE, Kao R, Wheeler J, Gogate J, Opal SM. Phase 2 trial of eritoran tetrasodium (E5564), a toll-like receptor 4 antagonist, in patients with severe sepsis. Crit Care Med. 2010; 38(1):72–83. [PubMed: 19661804]
5. Afshari A, Wetterslev J, Brok J, Moller AM. Antithrombin III for critically ill patients. Cochrane Database Syst Rev. 2008; (3):CD005370. [PubMed: 18646125]
6. Marti-Carvajal AJ, Sola I, Lathyris D, Cardona AF. Human recombinant activated protein C for severe sepsis. Cochrane Database Syst Rev. 2011; (4):CD004388. [PubMed: 21491390]
7. Mei SH, Haitsma JJ, Dos Santos CC, Deng Y, Lai PF, Slutsky AS, Liles WC, Stewart DJ. Mesenchymal stem cells reduce inflammation while enhancing bacterial clearance and improving survival in sepsis. Am J Respir Crit Care Med. 2010; 182(8):1047–57. [PubMed: 20558630]
8. Matthay MA, Goolaerts A, Howard JP, Lee JW. Mesenchymal stem cells for acute lung injury: preclinical evidence. Crit Care Med. 2010; 38(10 Suppl):S569–73. [PubMed: 21164399]
9. Dhanireddy S, Altemeier WA, Matute-Bello G, O'Mahony DS, Glenny RW, Martin TR, Liles WC. Mechanical ventilation induces inflammation, lung injury, and extra-pulmonary organ dysfunction in experimental pneumonia. Lab Invest. 2006; 86(8):790–9. [PubMed: 16855596]
10. Barbier F, Andremont A, Wolff M, Bouadma L. Hospital-acquired pneumonia and ventilator-associated pneumonia: recent advances in epidemiology and management. Curr Opin Pulm Med. 2013; 19(3):216–28. [PubMed: 23524477]
11. Jones RN. Microbial etiologies of hospital-acquired bacterial pneumonia and ventilator-associated bacterial pneumonia. Clin Infect Dis. 2010; 51(Suppl 1):S81–7. [PubMed: 20597676]
12. Bolstad BM, Irizarry RA, Astrand M, Speed TP. A comparison of normalization methods for high density oligonucleotide array data based on variance and bias. Bioinformatics. 2003; 19(2):185–93. [PubMed: 12538238]
13. Fellenberg K, Hauser NC, Brors B, Neutzner A, Hoheisel JD, Vingron M. Correspondence analysis applied to microarray data. Proc Natl Acad Sci U S A. 2001; 98(19):10781–6. [PubMed: 11535808]
14. Kayala MA, Baldi P. Cyber-T web server: differential analysis of high-throughput data. Nucleic Acids Res. 2012; 40:W553–9. Web Server issue. [PubMed: 22600740]

15. Benjamini Y, Hochberg Y. Controlling the false discovery rate: a practical and powerful approach to multiple testing. Journal of the Royal Statistical Society. Series B. Methodological. 1995; 57:289–300.

16. Subramanian A, Tamayo P, Mootha VK, Mukherjee S, Ebert BL, Gillette MA, Paulovich A, Pomeroy SL, Golub TR, Lander ES, Mesirov JP. Gene set enrichment analysis: a knowledge-based approach for interpreting genome-wide expression profiles. Proc Natl Acad Sci U S A. 2005; 102(43):15545–50. [PubMed: 16199517]

17. Calvano SE, Xiao W, Richards DR, Felciano RM, Baker HV, Cho RJ, Chen RO, Brownstein BH, Cobb JP, Tschoeke SK, Miller-Graziano C, Moldawer LL, Mindrinos MN, Davis RW, Tompkins RG, Lowry SF. A network-based analysis of systemic inflammation in humans. Nature. 2005; 437(7061):1032–7. [PubMed: 16136080]

18. Jensen LJ, Kuhn M, Stark M, Chaffron S, Creevey C, Muller J, Doerks T, Julien P, Roth A, Simonovic M, Bork P, von Mering C. STRING 8--a global view on proteins and their functional interactions in 630 organisms. Nucleic Acids Res. 2009; 37:D412–6. Database issue. [PubMed: 18940858]

19. Seok J, Warren HS, Cuenca AG, Mindrinos MN, Baker HV, Xu W, Richards DR, McDonald-Smith GP, Gao H, Hennessy L, Finnerty CC, Lopez CM, Honari S, Moore EE, Minei JP, Cuschieri J, Bankey PE, Johnson JL, Sperry J, Nathens AB, Billiar TR, West MA, Jeschke MG, Klein MB, Gamelli RL, Gibran NS, Brownstein BH, Miller-Graziano C, Calvano SE, Mason PH, Cobb JP, Rahme LG, Lowry SF, Maier RV, Moldawer LL, Herndon DN, Davis RW, Xiao W, Tompkins RG. Inflammation and L. S. C. R. P. Host Response to Injury: Genomic responses in mouse models poorly mimic human inflammatory diseases. Proc Natl Acad Sci U S A. 2013; 110(9):3507–12. [PubMed: 23401516]

20. Takao K, Miyakawa T. Genomic responses in mouse models greatly mimic human inflammatory diseases. Proc Natl Acad Sci U S A. 2015; 112(4):1167–72. [PubMed: 25092317]

21. The Acute Respiratory Distress Syndrome Network. ARDSnet: Ventilation with lower tidal volumes as compared with traditional tidal volumes for acute lung injury and the acute respiratory distress syndrome. N Engl J Med. 2000; 342(18):1301–8. [PubMed: 10793162]

22. Luscombe NM, Babu MM, Yu H, Snyder M, Teichmann SA, Gerstein M. Genomic analysis of regulatory network dynamics reveals large topological changes. Nature. 2004; 431(7006):308–12. [PubMed: 15372033]

23. Vidal M, Cusick ME, Barabasi AL. Interactome networks and human disease. Cell. 2011; 144(6): 986–98. [PubMed: 21414488]

24. Gharib SA, Liles WC, Klaff LS, Altemeier WA. Noninjurious mechanical ventilation activates a proinflammatory transcriptional program in the lung. Physiol Genomics. 2009; 37(3):239–48. [PubMed: 19276240]

25. Fuchs BC, Hoshida Y, Fujii T, Wei L, Yamada S, Lauwers GY, McGinn CM, DePeralta DK, Chen X, Kuroda T, Lanuti M, Schmitt AD, Gupta S, Crenshaw A, Onofrio R, Taylor B, Winckler W, Bardeesy N, Caravan P, Golub TR, Tanabe KK. Epidermal growth factor receptor inhibition attenuates liver fibrosis and development of hepatocellular carcinoma. Hepatology. 2014; 59(4): 1577–90. [PubMed: 24677197]

26. Tang J, Liu N, Tolbert E, Ponnusamy M, Ma L, Gong R, Bayliss G, Yan H, Zhuang S. Sustained activation of EGFR triggers renal fibrogenesis after acute kidney injury. Am J Pathol. 2013; 183(1):160–72. [PubMed: 23684791]

27. Finigan JH, Downey GP, Kern JA. Human epidermal growth factor receptor signaling in acute lung injury. Am J Respir Cell Mol Biol. 2012; 47(4):395–404. [PubMed: 22652197]

28. Harada C, Kawaguchi T, Ogata-Suetsugu S, Yamada M, Hamada N, Maeyama T, Souzaki R, Tajiri T, Taguchi T, Kuwano K, Nakanishi Y. EGFR tyrosine kinase inhibition worsens acute lung injury in mice with repairing airway epithelium. Am J Respir Crit Care Med. 2011; 183(6):743–51. [PubMed: 20935109]

29. Clark JA, Clark AT, Hotchkiss RS, Buchman TG, Coopersmith CM. Epidermal growth factor treatment decreases mortality and is associated with improved gut integrity in sepsis. Shock. 2008; 30(1):36–42. [PubMed: 18004230]

30. Dominguez JA, Vithayathil PJ, Khailova L, Lawrance CP, Samocha AJ, Jung E, Leathersich AM, Dunne WM, Coopersmith CM. Epidermal growth factor improves survival and prevents intestinal

injury in a murine model of pseudomonas aeruginosa pneumonia. Shock. 2011; 36(4):381–9. [PubMed: 21701422]

31. Qi WX, Fu S, Zhang Q, Guo XM. Incidence and risk of severe infections associated with anti-epidermal growth factor receptor monoclonal antibodies in cancer patients: a systematic review and meta-analysis. BMC Med. 2014; 12:203. [PubMed: 25369798]
32. Gharib SA, Khalyfa A, Abdelkarim A, Ramesh V, Buazza M, Kaushal N, Bhushan B, Gozal D. Intermittent hypoxia activates temporally coordinated transcriptional programs in visceral adipose tissue. J Mol Med (Berl). 2012; 90(4):435–45. [PubMed: 22086141]

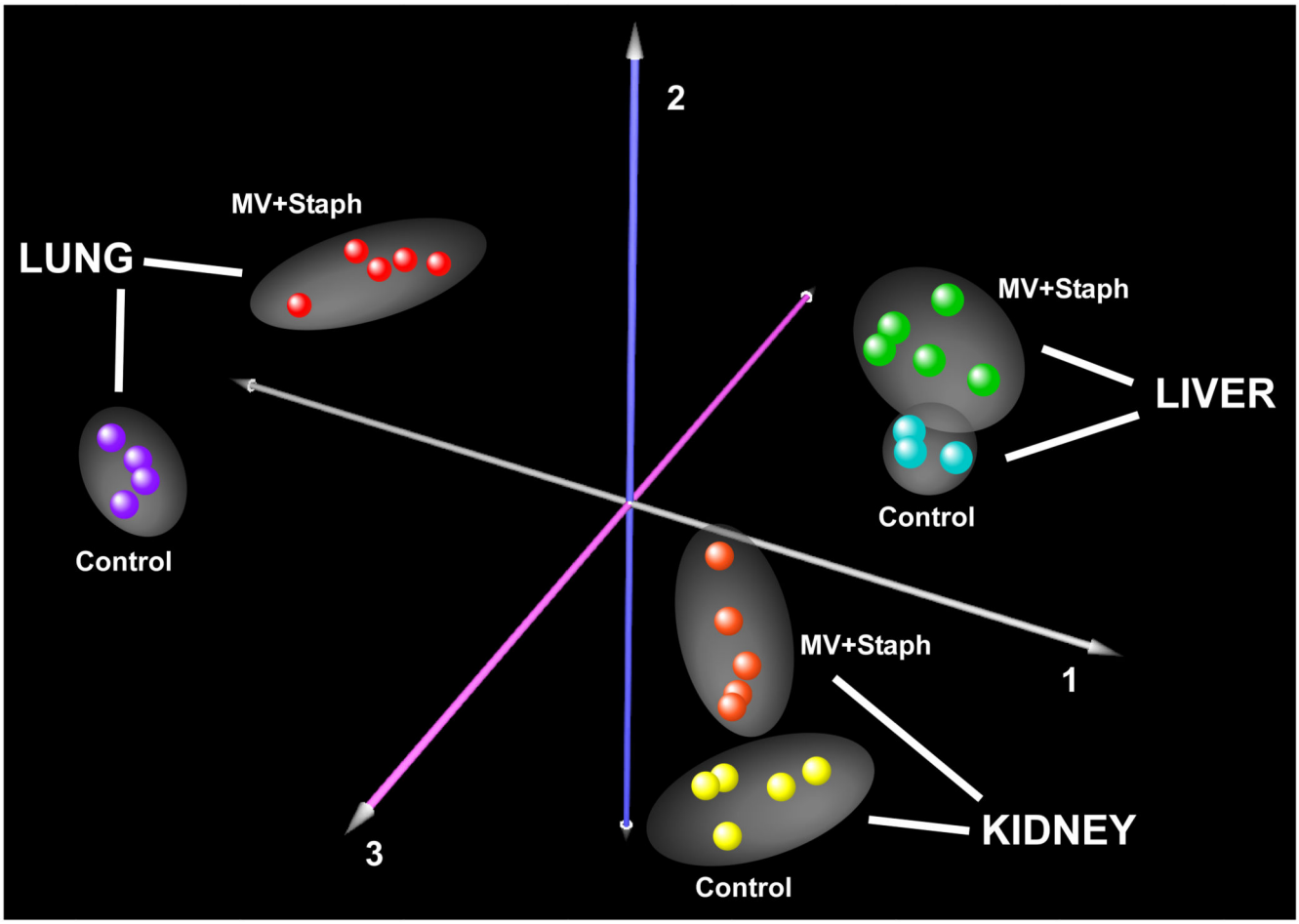

Figure 1.

Correspondence analysis of multi-organ transcriptional profiles in experimental SIRS. This analysis segregated samples (n = 27) based on gene expression variability due to sample replication, experimental exposure (MV+SA, Control), and organ type (lung, liver, kidney). Each orthogonal axis captured a fraction of total expression variability. Note that the samples separated primarily based on organ type followed by exposure condition; as expected, the least contributor to gene expression variability was sample replication.

Figure 2.

Organ-specific gene set enrichment profiles in SIRS. Transcriptional responses of lung, liver, and kidney to MV+SA were analyzed using GSEA, leading to identification of common and divergent pathways. Representative gene sets are labeled and the complete list is provided in Supplementary Table S1. A common core of pathways enriched across organs was identified and selected for subsequent analysis (please see Figure 3).

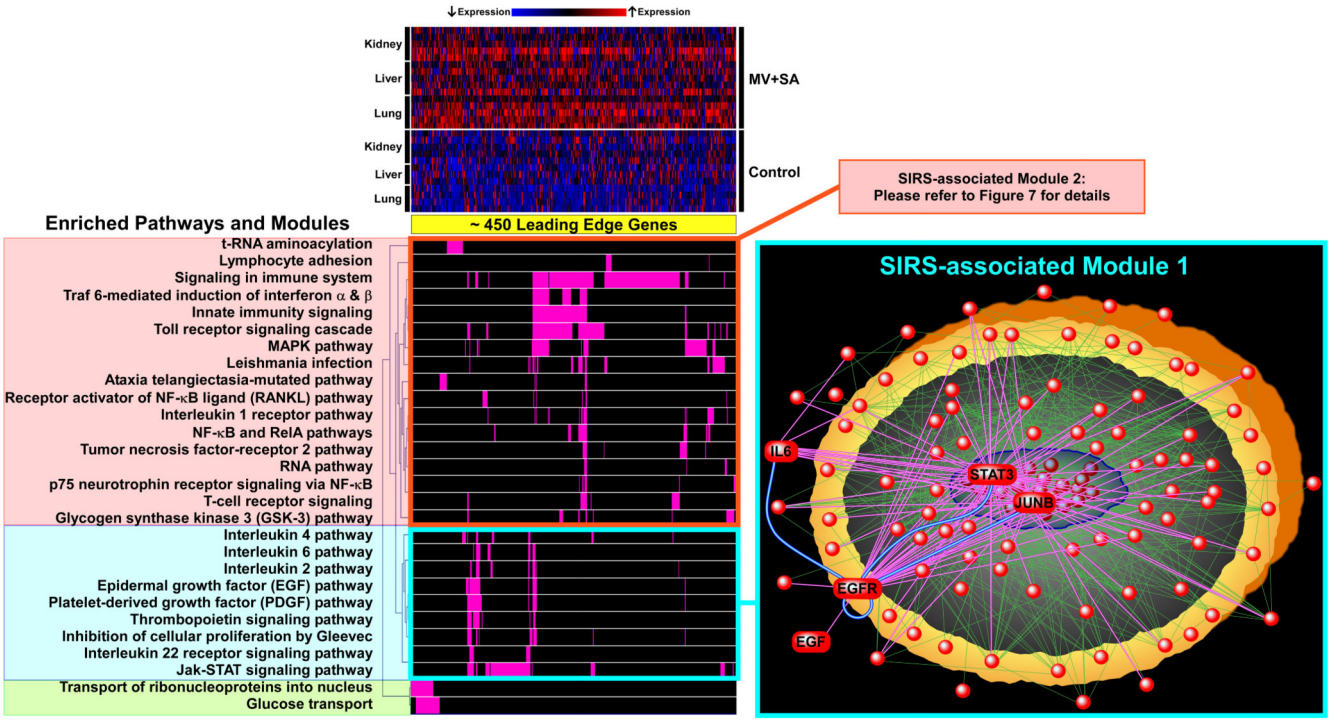

Figure 3.

Graphical representation of organ-spanning, SIRS-associated genes, pathways, biologic modules and networks. The expression profile of approximately 450 leading edge genes driving SIRS is depicted as a heatmap and demonstrates upregulation of most genes across organs during exposure to MV+SA. Commonly enriched gene sets (see Figure 2) were clustered together into larger modules based on the membership profile of their corresponding leading edge genes. The largest cluster of pathways mapped to well-recognized immuno-inflammatory processes involved in sepsis including Toll receptor signaling, innate immunity, Tnf signaling, and the NF-κB cascade (Module 1). Another distinct module comprised of interleukin, EGF, PDGF, and Jak-STAT signaling pathways was identified and the relationships among its components mapped using network analysis (Module 2, complete list of nodes provided in Supplementary Table S2). The topology of this SIRS-associated network was characterized by several densely connected nodes, most prominently, EGFR, but also STAT3, JUNB, and IL6. As the most densely interacting node, EGFR represented a hub of connectivity across the network (magenta lines).

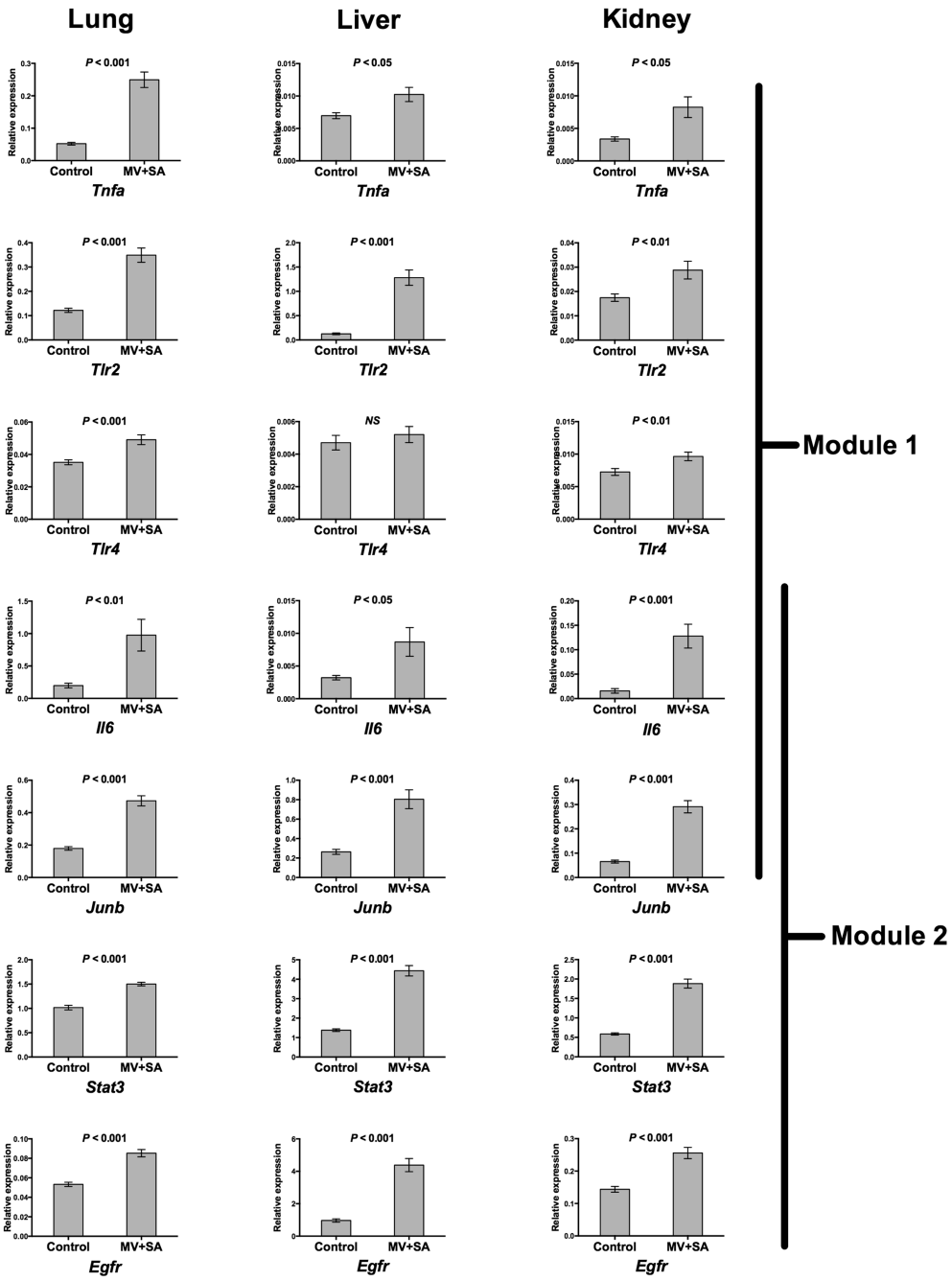

Figure 4.

Quantitative PCR confirmation of microarray results. Using an independent set of control (n = 6) and MV+SA (n = 6) experiments, we validated the differential upregulation of several key genes in Modules 1 and 2 including *Tnfa*, *Tlr2*, *Tlr4*, *Il6*, *Junb*, *Stat3*, and *Egfr* in multiple organs during SIRS. Note that *Il6* and *Junb* were members of both Modules. Data represent mean relative expression ± SEM. *P*-values for differences between means were calculated using two-tailed Student's *t*-test.

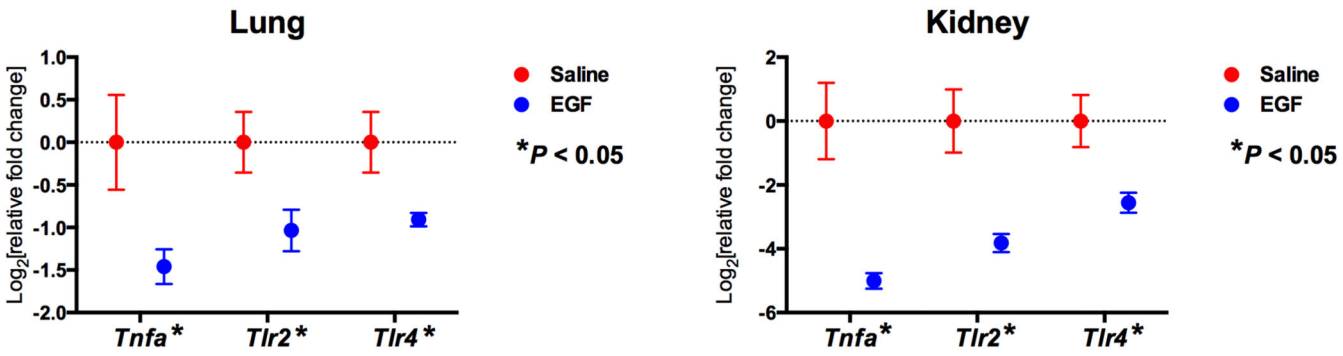

Figure 5.

Transcriptional effects of exogenous murine EGF (mEGF) on selected Module 1 nodes during SIRS. mEGF administered to mice exposed to MV+SA significantly down-regulated several key immuno-inflammatory genes (*Tnfa*, *Tlr2*, *Tlr4*), implying that targeting the EGF-EGFR axis in Module 2 influences the transcriptional response of Module 1. Data represent mean relative expression ± SEM. *P*-values for differences between means were calculated using two-tailed Student's *t*-test. *$P \leq 0.05$.

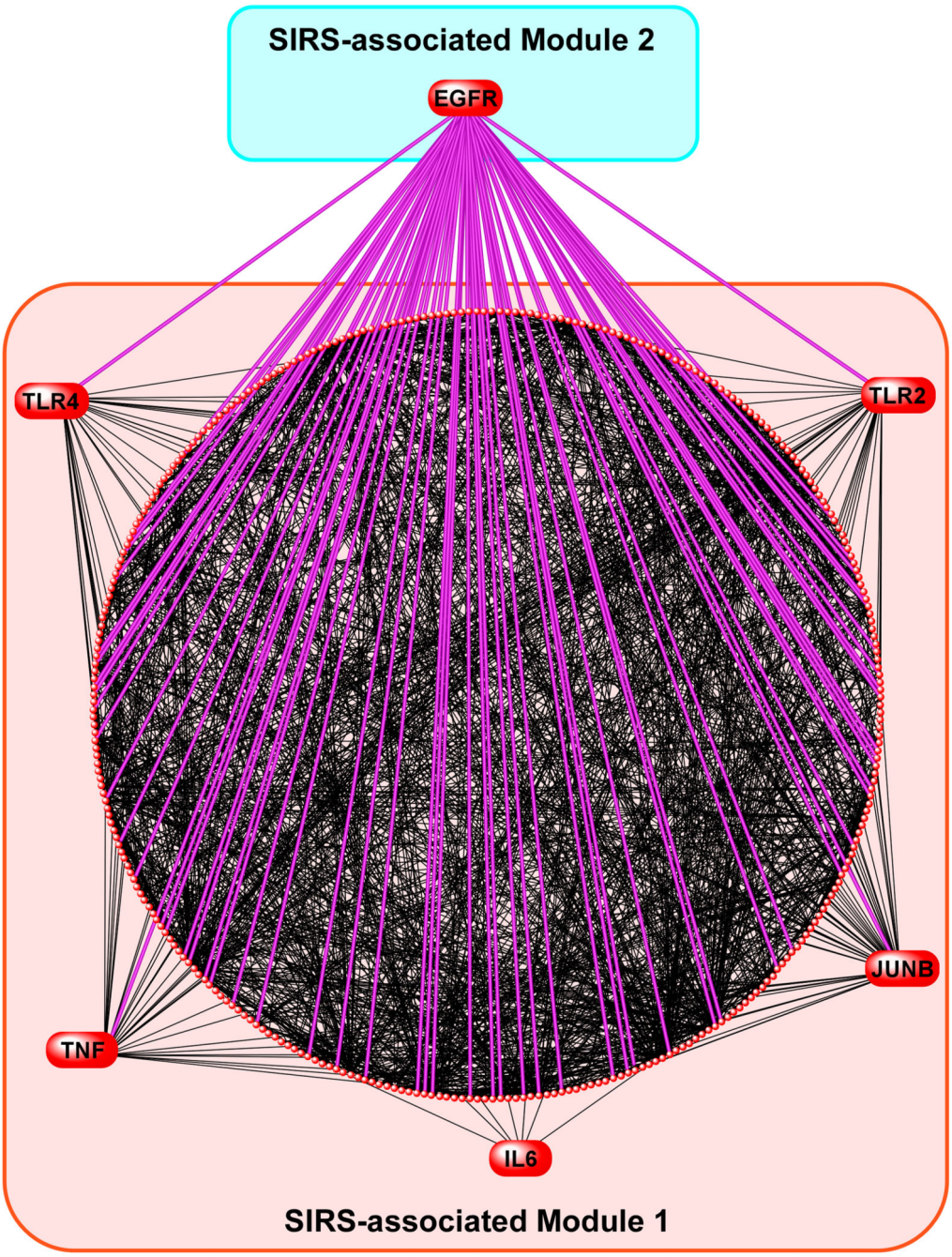

Figure 6.

Interconnectivity of EGFR (a Module 2 hub) with Module 1 genes. Harnessing gene product interaction databases we developed a relational network for Module 1 nodes and their interactions with EGFR. The diffuse connectivity between EGFR and members of the network implies that robust intermodular influences are mediated through the EGF-EGFR axis in SIRS and precede development of MODS.